Tunable Field Imbalance and Spin Precession in Magnetic Double Layers

Y. Au and R. Sooryakumar

Department of Physics, The Ohio State University, Columbus, OH 43210

K. Bussmann

Naval Research Laboratory, Washington DC 20375.

We report on the manipulation of spin-wave mode profiles by a field *imbalance* in magnetic double layers produced by the combination of an external field (H_{ext}) and an in-plane spacer layer current-induced Amperian field (H_{cur}). The magnetizations between layers are tuned from anti-parallel to parallel alignment and the associated oscillation amplitudes monitored by Brillouin light scattering. While the results are well accounted for by Maxwell and Landau-Lifshitz equations, a mechanical coupled pendulum analog in a variable unbalanced gravitational acceleration (Δg) provides insight into the underlying physics. It is pointed out that application of magnetic field *pulses* of specific strength and duration will lead to direct cross-communication between spin-wave normal modes, a feature unique to the tunable local imbalanced field.

Thin ferromagnetic/ normal metal multilayer structures have received much attention over the last two decades and have emerged as magnetic field sensors, computer hard-disk read heads and magnetic random access memory elements[1]. Although initially the current density for these applications was retained at modest levels, it has been raised to values beyond 10^7 A/cm^2 in order to enhance signals[2], produce controlled movement of domain walls[3] and create measurable spin-torque transfer between magnetic layers.[4] In these studies attention was largely focused on the influence of the current on the *static* component of the magnetization for memory applications. As witnessed by the recent discovery of micro-wave emission from structures in a current perpendicular to plane (CPP) geometry[5] there is growing interest in exploring the *dynamic* magnetization component. The microwave emission in these systems has led to suggestions that it could be utilized in mesoscopic oscillators and electronic clocks. Such technologies would require more detailed understanding of the interactions between the dynamic components of the magnetization and the required high current densities. While these investigations have generally been limited to the spin-torque transfer mechanism, the impact of the Amperian self-magnetic field (H_{cur}) associated with the current on the precessing magnetization has received little attention. Interestingly, for a current-in-plane (CIP) geometry, an external in-plane field (H_{ext}) together with such Amperian fields at current density values of ~10^7 A/ cm^2 fall in a range that generates a spatial field imbalance within a multilayer structure to dramatically modify the oscillation profile of the magnetization. In this paper, we present a Brillouin light scattering (BLS) study providing direct measure of such local variations of the *dynamic* magnetization components in distinct, spatially separated, layers. The results, while in agreement with first principle calculations, are also analyzed within a mechanical analog of a coupled pendulum in an unbalanced gravitational field.

The permalloy-copper-permalloy tri-layers of $Ni_{80}Fe_{20}(d)/Cu(d_0)/Ni_{80}Fe_{20}(d)$ (nominally d=30nm, d_0=45nm) were sputter-deposited on two diamond substrates (sample #1 and #2), followed by photolithography and wet etched to yield patterned channels of width and length 50x100μm (sample #1) and 75x150 μm (sample #2).[6] The current $I_{channel}$ that flows primarily through the spacer copper layer was introduced via leads placed outside the channel and current densities as high as 4×10^7 A/cm^2 were realized. The resulting Amperian field H_{cur} is oriented along opposite directions in each permalloy layer. H_{cur} hence either augments or diminishes the in-plane external field H_{ext} applied perpendicular to the direction of current flow thereby creating a field imbalance $|H_{ext}+H_{cur}|$ and $|H_{ext}-H_{cur}|$ at each magnetic layer as shown in Fig. 1. The precessing moments illustrated in Fig. 1 depict the in-phase surface acoustic (SA) and out-of-phase surface optic (SO) spin-waves (SW) for different directions of current flow and relative magnitudes of H_{ext} and H_{cur}.

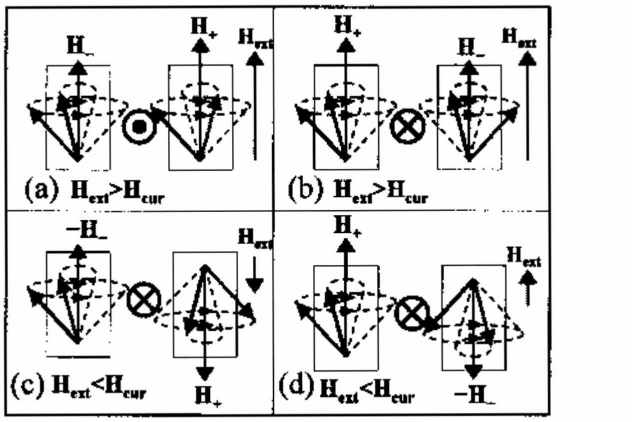

FIG. 1 Schematic illustration of in- and out-of- phase magnetization oscillations shown respectively as black and grey arrows on precession cones for various Amperian (H_{cur}) and external field (H_{ext}) directions and magnitude. The rectangles represent the two magnetic layers in cross-section. For (a) and (b) $|H_{ext}| > |H_{cur}|$, while in (c) and (d) $|H_{ext}| < |H_{cur}|$.

The probe laser beam is incident from the left and directions of $I_{channel}$ indicated by ⊗ and ⊙ while $H_{\pm}=H_{ext}\pm H_{cur}$.

The SWs were detected by Brillouin ($p \rightarrow s$) scattering and recorded as a function of $I_{channel}$ in backscattering utilizing 70mW of 514.5nm radiation at 25K (to minimize Joule heating effects). In relation to Fig. 1, all BLS scans were measured with the probe beam incident from the left.

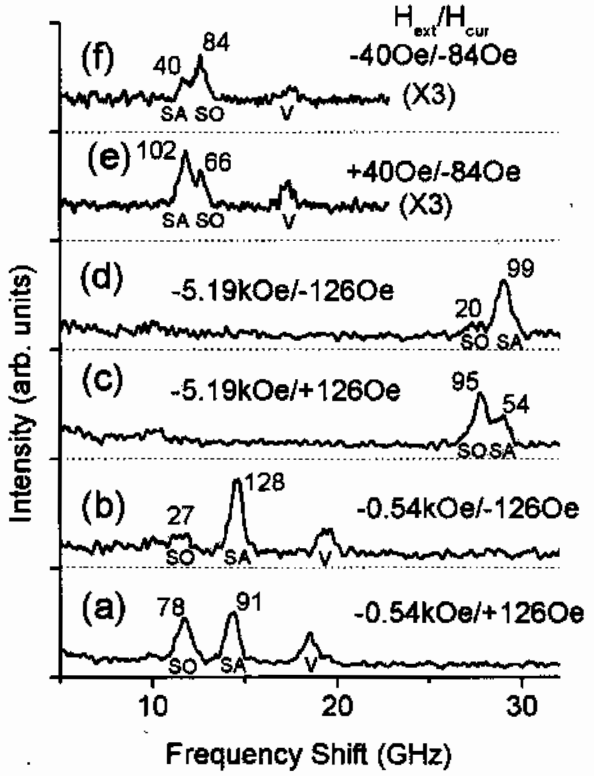

FIG. 2 Anti-Stokes Brillouin spectra recorded in sample #2 for various values of H_{ext} and H_{cur} ($I_{channel}$). The numbers beside each peak indicate the peak intensity (subtracted from background). All spectra are recorded with light incident on same magnetic layer.

Figs. 2a-f show representative anti-Stokes Brillouin spectra for different H_{ext} and H_{cur} (derived from $I_{channel}$ and channel width) taken on sample #2. Three peaks, SO, SA and the volume mode (V) are identified based on Maxwell and Landau-Lifshitz equations.[6] The spectrum in Fig. 2a corresponds to the dynamic magnetization amplitudes depicted in Fig. 1a with parallel alignment of M_1 and M_2 (magnetizations of the two permalloy layers). Here the SW amplitude of the SA (SO) mode is suppressed (enhanced) from its zero $I_{channel}$ value (not shown) in the left ferromagnetic layer on which the probe laser beam is incident. In the spectrum of Fig. 2b, H_{cur} ($I_{channel}$) is reversed. This corresponds to Fig. 1b, where now the SA (SO) amplitude is instead enhanced (suppressed) from its zero $I_{channel}$ value. These changes to the SW amplitudes in Fig. 1a and b are consistent with the observed changes of SA to SO BLS peak ratio from Fig. 2a (91/78=1.1) to Fig. 2b (128/27=4.7). Fig. 2c and 2d present similar spectra at a much higher external field (H_{ext}=-5.19kOe) and the SO/SA peak intensity switching feature complies with those of Fig. 2a and 2b. Fig. 2e illustrates a BLS spectrum at a regime where $|H_{cur}| > |H_{ext}|$. In this case the Stokes surface SW frequencies (not shown) do not match their anti-Stokes counterpart confirming anti-parallel alignment of M_1 and M_2 as in Fig. 1c. Finally when H_{ext} is reversed with H_{cur} unchanged, the intensity switching evident in Fig. 2f corresponds to the case in Fig. 1d.

In order to quantify the dependence of the mode intensity switching on the effective magnetic field, we define the switching strength parameter S at each value of $|H_{ext}|$ and $|H_{cur}|$, given by $S(|H_{ext}|,|H_{cur}|)$ = R(same) / R(opposite).[7] Here R(same) and R(opposite) are the peak intensity ratios of the higher (ω_h) to lower (ω_ℓ) frequency surface SW in the BLS spectrum when H_{ext} and H_{cur} are respectively directed in the same and opposite directions on the magnetic layer on which the probe laser beam is incident. Fig. 3 summarizes the measured data (from both sample #1 and #2) with calculated fits based on Maxwell and Landau-Lifshitz equations of the switching strength S as a function of $|H_{ext}|$ for different values of $|H_{cur}|$. The calculation adopted M_0 (saturation magnetization) = 774Oe, d = 32.2nm and d_0 = 45nm to achieve the best agreement with observed SW frequencies and the parameter S. It is noted from Fig. 3 that for anti-parallel alignment ($|H_{ext}| < |H_{cur}|$) of M_1 and M_2, calculations show that as $|H_{ext}|$ increases S rises on a single curve for different Amperian fields $|H_{cur}|$. On the other hand, as $|H_{ext}|$ is swept beyond this range, S sequentially collapses to values corresponding to parallel alignment when $|H_{ext}|$ surpasses $|H_{cur}|$. The switching ratio now lies on separate curves for different $|H_{cur}|$ with the curves remaining relatively flat for $|H_{ext}|$ < 1kOe and subsequently rising gradually with $|H_{ext}|$ beyond 1kOe (curves with larger $|H_{cur}|$ display greater rate of increase). These trends of the dependence of S on $|H_{ext}|$ and $|H_{cur}|$ are also reflected fairly well in the experimental data (Fig. 3).

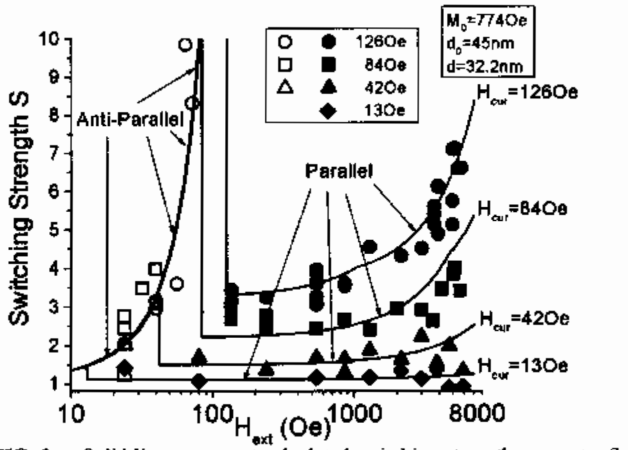

FIG. 3 Solid lines represent calculated switching strength parameter S as a function of $|H_{ext}|$ for various values of $|H_{cur}|$. An experimental point is hollow (filled) if spectra correspond to anti-parallel (parallel) alignment of magnetization is detected.

In order to gain physical insight into the results summarized in Fig. 3 we introduce a mechanical analog of M_1 and M_2, namely a coupled pendulum (spring constant k) (Fig. 4a) where the two masses (m) experience different gravitational fields g+Δg and g-Δg. Setting α=k/m and seeking solutions in the form $x_\sigma = \rho_\sigma e^{i\omega t}$ the eigenvalues and eigenvectors for the pendulum normal mode are respectively $\omega^2 = g + \alpha \mp \sqrt{\alpha^2 + \Delta g^2}$ and

$$\begin{bmatrix} \rho_1 \\ \rho_2 \end{bmatrix} = \frac{1}{\sqrt{1+f_{\mp}^2(\eta)}} \begin{bmatrix} f_{\mp}(\eta) \\ 1 \end{bmatrix}$$

where $f_{\mp} = -\eta \pm \sqrt{1+\eta^2}$ and η=$\Delta g/\alpha$. Fig. 4b and c show the dependence of ρ_1 and ρ_2 on η for the low (l) and high (h) frequency normal modes respectively. It is noted that the eigenvectors solely depend on the ratio $\Delta g/\alpha$ (= η), and are *independent* of g.

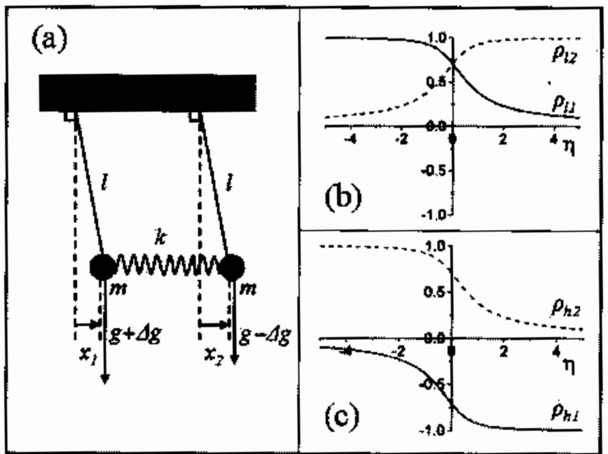

FIG. 4 (a) Coupled pendulums with different local gravitational fields (g+Δg) and (g-Δg). (b) and (c) illustrate dependence of normalized eigenvector elements ρ_1 and ρ_2 on η (=$\Delta g/\alpha$) for the lower (l) and higher (h) frequency normal modes.

In an anti-parallel alignment configuration, H_{cur} and H_{ext} are equivalent to g and Δg respectively. Therefore, in analogy to the pendulum eigenvectors, modifications to the SW mode amplitudes, and thus the parameter S, are independent of H_{cur} and depend only on H_{ext}. This accounts for the rise of S on a single curve for different H_{cur} in Fig. 3 in the anti-parallel region. On the other hand, since H_{ext} and H_{cur} switch roles in being represented by g and Δg when transiting from anti-parallel to parallel alignment, after the transition S does not depend on H_{ext} (equivalent to g) anymore but is now sensitive only to H_{cur} (Δg). Therefore, in Fig. 3, after entering parallel alignment (for H_{ext} < 1kOe) S transfers to a distinct set of flat curves for different H_{cur}. The gradual increase of S beyond H_{ext} > 1kOe in Fig. 3 is explained in terms of the frequency splitting between the SA and SO modes. Fig. 2 shows that the frequency splitting decreases from 2.9GHz (Fig. 2a and b) to 1.5GHz (Fig. 2c and d) as $|H_{ext}|$ increases from 0.54kOe to 5.19kOe. A decrease in (ω_h - ω_ℓ) indicates a drop in the value of α which results in larger η (=$\Delta g/\alpha$) for a given value of Δg. Fig. 4b and c illustrates that a larger η corresponds to larger deviation of $\rho_{h1(2)}$ and $\rho_{l1(2)}$ from their η=0 values which would lead to a larger switching strength S. On the other hand, there exists a discontinuous jump of the surface SW frequency splitting that accompanies the anti-parallel to parallel transition (0.9GHz of Fig. 2e and f to 2.9GHz of Fig. 2a and b). This explains the abrupt drop of S across the anti-parallel/parallel boundary in Fig. 3.

Interesting results associated with "cross-communication" between the normal modes emerge when current *pulses*, rather than continuous channel currents are utilized. In the pendulum analogy, it can be shown that when the *constant* Δg in Fig. 4 is replaced by a field *pulse* of strength Δg and time duration Δt, the amplitude of the higher and lower frequency eigen-modes after passage of the pulse are, in general, a linear combination of the amplitudes of these two modes prior to the pulse. However for $\Delta g >> \alpha$ (η >>1) if the duration and height of the pulse is tailored to satisfy: 1) $\Delta t = \pi/(\omega_h - \omega_\ell)$ and 2) ω_ℓ = $[n/(n+1)]\omega_h$,[8] where ω_h (ω_ℓ) are the frequency of higher (lower) modes during application of the Δg pulse and n is an integer, then the lower and higher frequency mode will neatly exchange their amplitudes (instead of remaining in the aforementioned mixed state) after passage of the Δg pulse, thus achieving cross-communication between vibrational eigen-modes. Given that the eigenvectors do not depend on g, it follows that similar cross-communication between modes will not occur if a g-pulse replaces the Δg-pulse. Therefore, this mode cross-communication represents a dynamic mechanism that is unique to the coupled SW system with the freedom to tune the field imbalance.

In summary, we have investigated through Brillouin light scattering the effects of magnetic field imbalances on the precessional amplitudes of SWs in a magnetic double layer. The imbalance, generated by an Amperian field and an external field, allows for the eigen-modes of the precessing magnetizations to be locally tuned. The results are explained by conventional electrodynamics and within a mechanical coupled pendulum analog in an unequal gravitational field. Transfer of amplitude information from one mode to another by pulsed fields (equivalent to Δg-pulses), i.e. the cross-communication between SWs, is shown to be a distinctive feature of the tunable unbalanced local fields.

Work at The Ohio State University was supported by the NSF under grant DMR 0205521 and at the Naval Research Laboratory by the Office of Naval Research.

1. P. Grünberg, Phys. Today **54**(5), 31 (2001).
2. A. B. Kos, S. E. Russek, Y. K. Kim and R. W. Cross, IEEE Trans. Magn. **33**, 3541 (1997)
3. J. Grollier, P. Boulenc, V. Cros, A. Hamzić, A. Vaurès and A. Fert, Appl. Phys. Lett. **83**, 509 (2003)
4. L. Berger, Phys. Rev. B **54**, 9353 (1996); J. C. Slonczewski, J. Magn. Magn. Mater. **159**, L1 (1996)
5. M. Tsoi, V. Tsoi, J. Bass, A. G. M. Jansen and P. Wyder, Phys. Rev. Lett. **89**, 246803 (2002); S. I. Kiselev, J. C. Sankey, I. N. Krivorotov, N. C. Emley, R. J. Schoelkopf, R. A. Buhrman and D. C. Ralph, Nature **425**, 380 (2003); W. H. Rippard, M. R. Pufall, S. Kaka, S. E. Russek and T. J. Silva, Phys. Rev. Lett. **92**, 027201 (2004)
6. Y. Au, R. Sooryakumar and K. Bussmann, Phys. Rev. B **67**, 214409 (2003)

7 Note that absolute intensity values from different Brillouin spectra are not exactly comparable. The parameter S is defined to be insensitive to such variations. We impose the constraint 0.25 < R< 4.00 to account for the intensity resolution in our BLS spectra.

8.Since $\omega_h(\omega_l)$ monotonically increase(decrease) with Δg, the condition on the frequencies can be satisfied by merely tuning the magnitude of Δg.